JACS
JOURNAL OF THE AMERICAN CHEMICAL SOCIETY

ARTICLE

pubs.acs.org/JACS

Radical Conversion and Migration in Electron Capture Dissociation

Benjamin N. Moore, Tony Ly, and Ryan R. Julian

Department of Chemistry, University of California, Riverside, California 92521, United States

Supporting Information

ABSTRACT: Electron capture dissociation (ECD) is an important analytical technique which is used frequently in proteomics experiments to reveal information about both primary sequence and post-translational modifications. Although the utility of ECD is unquestioned, the underlying chemistry which leads to the observed fragmentation is still under debate. Backbone dissociation is frequently the exclusive focus when mechanistic questions about ECD are posed, despite the fact that numerous other abundant dissociation channels exist. Herein, the focus is shifted to side chain loss and other dissociation channels which offer clues about the underlying mechanism(s). It is found that the initially formed hydrogen abundant radicals in ECD can convert quickly to hydrogen deficient radicals via a variety of pathways. Dissociation which occurs subsequent to this conversion is mediated by hydrogen deficient radical chemistry, which has been the subject of extensive study in experiments which are independent from ECD. Statistical analysis of fragments observed in ECD is in excellent agreement with predictions made by an understanding of hydrogen deficient radical chemistry. Furthermore, hydrogen deficient radical mediated dissociation likely contributes to observed ECD fragmentation patterns in unexpected ways, such as the selective dissociation observed at disulfide bonds. Many aspects of dissociation observed in ECD are easily reproduced in well-controlled experiments examining hydrogen deficient radicals generated by non-ECD methods. All of these observations indicate that when considering the means by which electron capture leads to dissociation, hydrogen deficient radical chemistry must be given careful consideration.

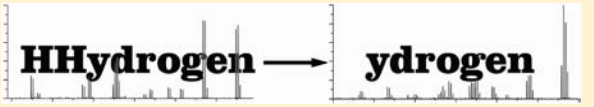

INTRODUCTION

Electron capture dissociation (ECD) and the related method electron transfer dissociation (ETD) continue to be important methods for extracting information in mass spectrometry based proteomics experiments.[1−5] These techniques are employed to obtain sequence information from peptides and proteins. Importantly, highly labile post-translational modifications are typically preserved during ECD/ETD,[6] which simplifies identification relative to collisional activation methods.[7] Technological developments have also enabled ECD/ETD to be used in high-throughput proteomic analyses, further increasing their utility.[8,9] Despite the value and popularity of ECD, the underlying mechanisms which dictate how fragmentation occurs are still not entirely clear and have been a subject for discussion over the last 10 years.[1,10−13]

Several of the mechanisms proposed for backbone dissociation in ECD proceed through an aminoketyl radical structure which dissociates into c and z$^{\bullet}$ ions, as shown in Scheme 1. Formation of c/z$^{\bullet}$ ions in ECD is analytically useful, due to the consistently high peptide sequence coverage in comparison to that of b/y ions generated by collision-induced dissociation (CID). Although the formation of the aminoketyl radical and subsequent dissociation into backbone fragments has been studied previously in detail,[14,15] less attention has been given to other dissociation channels which are commonplace in ECD. For example, a variety of neutral losses from the charge-reduced precursor ion are observed in ECD.[16−19] These neutral losses occur frequently and may provide additional insight into the mechanism of ECD which may not be apparent from an examination of backbone dissociation alone. Indeed, alternatives

Scheme 1. (a) Prototypical Backbone Dissociation into c/z$^{\bullet}$ Ions and (b) Migration of the Aminoketyl Radical

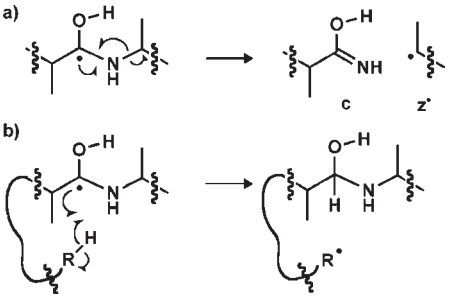

to c/z$^{\bullet}$ ion formation exist even for the aminoketyl radical itself, which can also potentially undergo radical migration, as shown in Scheme 1b. It has also been postulated that a radical cascade mechanism may be responsible for some of the fragmentation observed in ECD.[20] Radical cascade mechanisms require an initial backbone c/z$^{\bullet}$ dissociation and are similar in theory to dissociation observed from activation of z$^{\bullet}$ product ions.[21,22]

Neutral loss of amino acid side chains is not exclusive to ECD but is also prevalent in experiments involving what are referred to as "hydrogen deficient" radical species. Hydrogen deficient radicals are distinct in that they have one less hydrogen atom than a

Received: October 27, 2010
Published: April 15, 2011

   dx.doi.org/10.1021/ja1096804 | J. Am. Chem. Soc. 2011, 133, 6997–7006

peptide in a given charge state would typically have: i.e., $[(M\text{-}H)^{\bullet} + nH]^{n+}$. These radicals can be produced by various methods such as gas-phase photodissociation (PD),[23,24] CID of anions,[25] electron detachment dissociation,[26,27] electron-induced dissociation,[28] CID of nitroso-containing peptides,[29] CID of peroxycarbamates,[30] free radical initiated peptide sequencing (FRIPS),[31] dissociation of peptide−metal adducts,[32,33] and femtosecond laser pulses.[34] ECD itself also produces $c^{\bullet}$ and $z^{\bullet}$ type product ions which are hydrogen deficient radical species and behave as such.[16,35−40] Hydrogen deficient radical peptides generated by these methods typically yield amino acid side chain losses and $a/x^{\bullet}$ backbone fragmentation when subjected to CID or radiative heating.[41] ECD, on the other hand, typically produces $c/z^{\bullet}$ fragments and side chain losses, some of which are distinct to those observed in hydrogen deficient radical experiments.

A major hallmark of hydrogen deficient radical chemistry is radical migration, a process which allows the radical to travel to stable sites within the molecule.[42,43] In radical migration an initially formed hydrogen deficient radical abstracts a neighboring hydrogen atom through space, thus quenching one radical and creating a new one, as shown in Scheme 2a. Radical migration pathways allow a variety of side chain losses and backbone dissociations to occur at sites distant from the location of the initial radical. We have previously proposed that radical migration pathways in peptides and proteins are determined by the bond dissociation energies (BDEs) of available hydrogens as well as the constraints imposed by the gas-phase structure.[41] Migration is facilitated when the BDE of the radical acceptor site is comparable to or lower than the BDE of the radical donor. Conformational constraints must also allow proper alignment of the donor and acceptor in order for migration to occur. Under conditions where the relative BDE difference is favorable and structural constraints are negligible, barriers to migration are predicted to be quite small.[43,44] Typically we have found that the flexibility available in moderately sized peptides minimizes structural constraints such that the BDEs become good qualitative predictors of radical mobility.[41] This is not the case in whole proteins, where radical fragmentation is confined to spatially adjacent residues, although valuable structural information can be obtained in this fashion.[45]

At face value, backbone fragmentation and side chain losses from the charge-reduced precursor ion in ECD appear to be distinct from what is observed in hydrogen deficient radical experiments, because many of the products have been mass-shifted. Formally, fragmentation in ECD is initiated from a "hydrogen abundant" radical species, i.e. $[(M + H^{\bullet}) + nH]^{n+}$, which after charge reduction has one extra hydrogen atom relative to the canonical protonated species $[M + nH]^{n+}$. The hydrogen abundant product that is formed after electron capture becomes the initial structure leading to all observed ECD fragmentation. Electron capture, as proposed by McLafferty, Zubarev, and co-workers[1] in what is referred to as the Cornell mechanism, occurs directly at a protonated charge site, resulting in a hydrogen abundant radical species. This species can then donate a hydrogen atom to a backbone carbonyl to form the aminoketyl radical and subsequently undergo $c/z^{\bullet}$ type fragmentation. Charge remote electron capture, as proposed by Turecek[46] and Simons,[11,47] occurs by electron capture at a backbone carbonyl or disulfide to form an anionic species. Dissociation can then occur at the site of electron capture directly (Utah mechanism) or after proton transfer (Washington mechanism). Numerous charge remote capture pathways involving backbone or disulfide bond cleavage are frequently referred to collectively as the Utah−Washington mechanism. The Cornell and Washington mechanisms both involve conversion to a hydrogen deficient radical species; however, the possibility of radical migration within this species is not typically considered. For simplicity, we will adopt the formalism of direct electron capture at charged sites to describe chemistry related to hydrogen deficient radical migration in the present paper. *It should be understood that, in theory, all of the chemistry that will be described could also be initiated by charge remote electron capture followed by proton transfer.* Determining the extent to which this might occur in actual ECD is beyond the scope of this paper.

Scheme 2. Generic Mechanisms of (a) Hydrogen Deficient Radical Migration, Where the Radical and Hydrogen Atom Exchange Locations, (b) Hydrogen Abundant Radical Migration, Where the Radical and Hydrogen Atom Are Collocated, and (c) Radical Conversion from a Hydrogen Abundant to a Hydrogen Deficient State

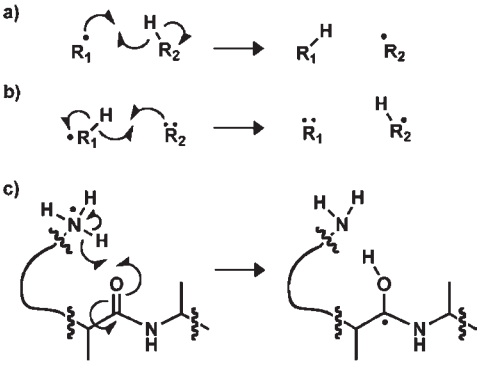

It is important to point out that hydrogen abundant radical species can also undergo radical migration, but not by the hydrogen atom abstraction process previously described for hydrogen deficient radicals. Instead, the excess hydrogen atom is transferred from the initial radical site to a hydrogen atom accepting site to form a new hydrogen abundant radical at that location, as shown in Scheme 2b. In this case, the radical and hydrogen atom are collocated and move in the same direction, which is in contrast with hydrogen deficient migration, where the hydrogen atom and radical migrate in opposite directions. This subtle difference in the mechanism of migration is an important characteristic in distinguishing hydrogen abundant and hydrogen deficient radical chemistry.

Hydrogen abundant radical migration should also not be confused with "radical conversion", where a hydrogen abundant radical is converted into a hydrogen deficient radical. An example is shown in Scheme 2c, where the aminoketyl radical, a hydrogen deficient product, is formed from the conversion of a hydrogen abundant precursor. Transfer of the abundant hydrogen from the charge-reduced hypervalent amine transforms the backbone carbonyl into an alcohol, thus converting the radical from hydrogen abundant to hydrogen deficient. A loss of a degree of saturation accompanies this process.

In this paper we demonstrate that hydrogen deficient radical chemistry plays an important role in much of the dissociation that is observed in ECD. Statistical analysis of a large body of ECD data suggests that the hydrogen-abundant species that are initially formed by electron capture quickly convert into hydrogen deficient radicals. This can occur via a variety of pathways;

the most common pathways are outlined herein. Photodissociation experiments designed to explore side chain dissociations observed in hydrogen-deficient radical peptides are reported. These experiments confirm that hydrogen deficient chemistry can rationalize similar fragmentations observed in ECD, including selective fragmentation observed at disulfide bonds. Understanding the role that radical chemistry plays in ECD provides significant insight into the mechanisms which are responsible for both backbone and side chain dissociation.

EXPERIMENTAL SECTION

The peptide RPPGYSPFR was purchased from American Peptide Co. (Sunnyvale, CA). This peptide was iodinated at tyrosine by a previously described method.[48] The carbon−iodine bonds of iodotyrosine-containing peptides were photodissociated in the gas phase by transmitting fourth harmonic (266 nm) laser light, generated from a flash-pumped Nd:YAG laser (Continuum, Santa Clara, CA), through a quartz window on the rear vacuum flange of a modified LTQ linear ion trap (ThermoFisher, Waltham, MA) as previously described.[23] α-Methylcysteine was purchased from Nagase Co. (Osaka City, Japan), Fmoc protected,[49] and acetamide protected. The peptides YVDIAIPCGNK and its α-methylcysteine derivative were synthesized by solid-phase peptide synthesis.[49] *S*-Cysteine-acetamide-containing peptides were derived from cysteine-containing peptides by reaction with an excess of iodoacetamide in water in the dark at 40 °C for 1 h.[50] Dehydroalanine-containing peptides were derived from phosphoserine-containing peptides by reaction with $Ba(OH)_2$ solution at 40 °C for 1 h.[51] Disulfide-bonded dipeptides were created by oxidizing two peptides, each containing a single free cysteine in the presence of DMSO, 20% by volume in water.[52] Each of these products was purified separately on a C8 peptide purification column and diluted to a concentration of 5 μM in 90/10/1 acetonitrile/water/acetic acid before being electrosprayed.

Chemical structure and energy calculations were performed with the Gaussian 03 Ver. 6.1 Rev. D.01 software package (Gaussian, Inc., Wallingford, CT).[53] All calculations used the hybrid density functional theory B3LYP with the 6-31G(d) basis set unless otherwise stated. The bond dissociation energies (BDE) of the neutral aminoketyl radical and Gln, Glu, Asp, and Asn side chain radicals were calculated by the isodesmic reaction method using the experimentally determined BDE of $H-CH_2OH$ (96.1 ± 0.2 kcal mol^{-1}) as a reference.[54] All other BDEs were calculated using appropriate reference energies. Transition states were determined by quasi-Newtonian synchronous transit (QST3) calculations and verified by visualization of the single imaginary frequency.[55]

Percentages of side chain loss in Table 1 were calculated on the basis of analysis of the SwedECD database and are similar to those which have been previously reported.[17] An algorithm was used which examined each peptide ECD spectrum in the database and looked for specific side chain losses by mass from the charge-reduced species. The number of peptides which contained the experimentally observed side chain loss and also contained the residue expected to generate the side chain loss were summed and then divided by the total number of peptides containing the residue. Finally, these values were converted to a percentage and compiled for all side chain losses in Table 1. Peptides containing amino acids with side chain losses that overlap by mass were excluded from the analysis when appropriate.

RESULTS AND DISCUSSION

Evidence for Hydrogen Deficient Chemistry. It is first necessary to determine whether any of the numerous dissociation pathways observed in ECD are best explained by hydrogen deficient radical chemistry. For a statistically relevant source of ECD data, we will use the SwedECD database made publicly available by the Zubarev group.[17] SwedECD contains 11 491 ECD mass spectra of peptides derived from a tryptic digest of cell lysates. From this database we can extract trends relating formation of certain product ions with amino acid identity, sequence length, and a variety of other parameters. Specific side chain losses from the charge-reduced species in ECD have been previously investigated for their analytical utility in the differentiation of isomeric sequences, improvement of database searching, and de novo sequencing.[17] In this work, however, side chain loss will be used to investigate the mechanistic details of ECD and its relation to hydrogen deficient radical chemistry. Only side chain loss from the charge-reduced parent ion in ECD is considered, since this is the product ion that results directly from electron capture and may initially contain a hydrogen abundant radical. Side chain losses from other products, such as $z^{\bullet}$ ions, have been examined previously and proceed through hydrogen deficient radical chemistry.[35] Table 1 shows side chain losses that are typically observed in both hydrogen abundant and hydrogen deficient radical experiments. At first glance, most of the hydrogen deficient/abundant side chain losses in Table 1 appear to be different from each other and unrelated. However, closer inspection and consideration is warranted, as will be detailed in the following sections.

Leucine Radical Side Chain Loss. The side chain loss of 56 Da from leucine is observed in both ECD experiments and when hydrogen deficient radicals are fragmented. However, simple observation of the same mass loss does not necessarily imply that the loss occurs via the same mechanism in both experiments; therefore, likely hydrogen abundant and hydrogen deficient pathways for the loss of 56 Da are considered in Scheme 3. The loss of 56 Da represents the mass of nearly the entire side chain; however, as shown in Scheme 3a, homolytic cleavage of the appropriate bond would actually result in a loss of 57 Da. Therefore, any correct mechanism will require the transfer of a hydrogen atom from the side chain to the peptide prior to dissociation. Hydrogen abundant dissociation typically involves attack by the excess hydrogen atom (see Scheme 2b), which is unlikely in the case of the leucine side chain due to the absence of favorable sites to receive the hydrogen atom. Furthermore, attack at the side chain would ultimately result in a loss of 58 Da, as shown in Scheme 3b, not the required 56 Da. Similarly, hydrogen atom attack at the α position would result in a loss of 57 Da, which is not acceptable either. Hydrogen abundant radical chemistry does not therefore offer a palatable explanation for the observed loss. In contrast, hydrogen deficient chemistry readily leads to this type of loss via the mechanism outlined in Scheme 3c.[36] If the initial hydrogen abundant parent ion underwent conversion to a hydrogen deficient species, then migration of that radical to the γ position of leucine would provide the required hydrogen transfer. Subsequent β dissociation would generate the observed loss of 56 Da. Consideration of all possible mechanisms suggests that this loss is actually generated by the same pathway in both ECD and hydrogen deficient radical experiments. Furthermore, it implies that significant conversion to a hydrogen deficient state capable of radical migration occurs within the charge-reduced parent ion in ECD.

***S*-Cysteine-Acetamide Side Chain Loss and Disulfide Bond Cleavage.** Another side chain loss observed in both ECD and hydrogen deficient radical experiments is the loss of the *S*-cysteine-acetamide side chain. In the SwedECD study, peptides were reacted with iodoacetamide to cap cysteine residues, thus forming *S*-cysteine-acetamide and preventing any possible

Table 1. Partial List of Observed Neutral Side Chain Losses from the Charge-Reduced Peptides in ECD and Observed Neutral Side Chain Losses from Hydrogen-Deficient Radical Peptides

ECD neutral side chain losses				hydrogen deficient radical side chain losses		
amino acid	chem formula	exact mass	% peptides with loss[c]	amino acid	chem formula	exact mass
Arg	$C_4H_{11}N_3$	101.0953	2.2	Arg	$C_4H_9N_3$	99.0796
Arg	CH_3N2	43.0296	14.3	Arg	$C_3H_8N_3$	86.0718
Asn	C_2H_5NO	59.0371	47.1[a]	Asn	CH_2NO	44.0136
Asn	$CH_2NO + NH_3$	61.0401	13.8	Asp	CHO_2	44.9977
Asp	$C_2H_4O_2$	60.0211	60.4[a]	Cys*	C_2H_4NO	58.0293
Asp	$CHO_2 + NH_3$	62.0242	2.7	Cys*	C_2H_4NOS	90.0014
Cys[b]	C_2H_4NO	58.0293	88.8	Gln	C_2H_4NO	58.0293
Cys[b]	$C_2H_4NO + NH_3$	75.0558	19.9	Gln	C_3H_5NO	71.0371
Cys[b]	$C_2H_4NOS + NH_3$	107.0279	56.3	Glu	$C_2H_3O_2$	59.0133
Cys[b]	C_2H_5NO	59.0371	43.2[a]	Glu	$C_3H_4O_2$	72.0211
Cys[b]	C_2H_4NOS	90.0014	42.3	His	$C_4H_4N_2$	80.0374
Gln	$C_2H_4NO + NH_3$	75.0558	14.8	His	$C_3H_3N_2$	67.0296
Gln	C_2H_5NO	59.0371	5.6[a]	Ile	C_2H_5	29.0391
Gln	C_3H_5NO	71.0371	3.9	Ile	C_4H_8	56.0626
Gln	$C_3H_5NO + NH_3$	88.1000	0.3	Leu	C_4H_8	56.0626
Glu	$C_2H_3O_2 + NH_3$	76.0393	21.3	Leu	C_3H_7	43.0584
Glu	$C_3H_4O_2 + NH_3$	89.0471	6.7	Lys	C_3H_8N	58.0657
Glu	$C_2H_4O_2$	60.0211	1.0[a]	Lys	C_4H_9N	71.0735
His	$C_4H_6N_2$	82.0531	38.4	Met	C_3H_6S	74.0190
Ile	$C_2H_5 + NH_3$	46.0651	7.2	Met	CH_3S	46.9955
Ile	$C_4H_8 + NH_3$	73.0891	2.6[a]	Met	C_2H_5S	61.0112
Ile	C_4H_8	56.0626	1.0[a]	Ser	CH_2O	30.0106
Ile	C_2H_5	29.0391	0.7	Thr	C_2H_4O	44.0262
Leu	$C_4H_8 + NH_3$	73.0891	11.9[a]	Trp	C_9H_7N	129.0578
Leu	$C_3H_7 + NH_3$	60.0849	11.6	Tyr	C_7H_6O	106.0419
Leu	C_4H_8	56.0626	4.7[a]			
Leu	C_3H_7	43.0584	1.4			
Met	$C_3H_6S + NH_3$	91.0456	17.7			
Tyr	C_7H_8O	108.0575	3.5			

[a] Peptides containing other residues that exhibit the exact same side chain loss by mass are excluded from these results. [b] Denotes *S*-cysteine-acetamide. [c] % peptides with loss only considers peptides which contain the residue and is calculated by finding the percentage of peptides which upon ECD give the corresponding side chain loss within ±0.01 Da.

disulfide bond formation (this is commonly done in proteomics experiments). As seen in Table 1, peptides containing modified cysteine have an ~42% probability of producing a loss of 90 Da in ECD experiments. This loss is therefore highly favored in ECD. Hydrogen deficient radical peptides containing modified cysteine have not been investigated previously. In order to provide context for comparison, several peptides were treated with iodoacetamide to cap the cysteine, iodinated at tyrosine, and converted into hydrogen deficient radicals by photoactivation. As shown in Figure 1a, collisional activation of $[(CDPGYIGSR)^{\bullet} + H]^{+}$ yields a dominant loss of 90 Da. As discussed previously, radical migration is influenced by both relative BDEs and peptide structure. The results in Figure 1a likely result from structural factors which favor migration of the radical to cysteine; nevertheless, it is clear that the loss of 90 Da can be highly favored under the proper conditions. It is anticipated that doubly protonated CDPGYIGSR will not have the same structure as the singly protonated ion, which should influence radical migration. Indeed, Figure 1b shows CID of the doubly charged peptide radical yields a loss of 90 Da, though several other dissociation channels are observed as well. The results in Figure 1 are similar to those obtained for several other peptides and confirm that the

Scheme 3. Leucine Side Chain Loss: (a) Homolytic Cleavage of the $C_\alpha - C_\beta$ Bond Results in 57 Da Loss; (b) Attack by Hydrogen Atom Results in Loss of 58 Da; (c) Abstraction of the γ-Hydrogen Yields the Observed Loss of 56 Da

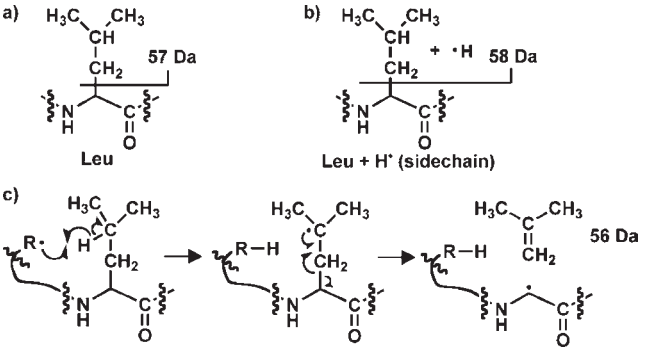

dx.doi.org/10.1021/ja1096804 |*J. Am. Chem. Soc.* 2011, 133, 6997–7006

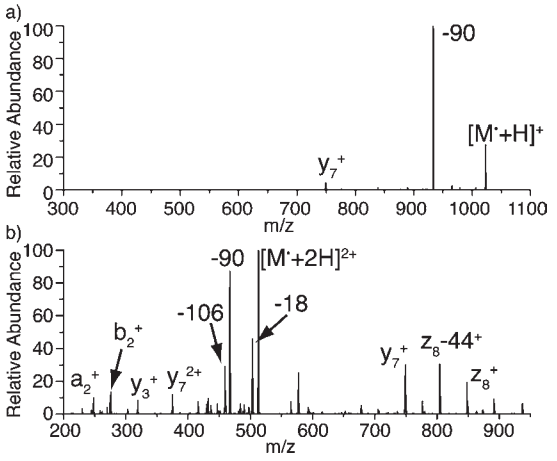

Figure 1. (a) PD/CID of singly charged $[(\text{cDPGYIGSR})^{\bullet} + \text{H}]^{+}$ and (b) PD/CID of doubly charged $[(\text{cDPGYIGSR})^{\bullet} + 2\text{H}]^{2+}$. The lower case "c" denotes the amino acid *S*-cysteine-acetamide.

Scheme 4. *S*-Cysteine-Acetamide Side Chain Loss: (a) Homolytic Cleavage of the C_β−S Bond Results in 90 Da Loss; (b) Hydrogen Atom Transfer to the β-Carbon Could Produce the 90 Da Loss; (c) Abstraction of the α-Hydrogen Yields the Experimentally Observed 90 Da Loss

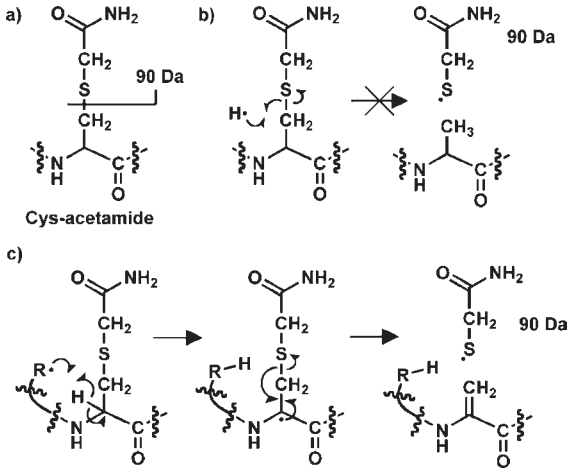

loss of 90 Da from modified cysteine is a favorable dissociation channel in hydrogen deficient radical peptides.

Possible mechanisms for the loss of 90 Da from modified cysteine are shown in Scheme 4. Homolytic cleavage of the C−S bond in *S*-cysteine-acetamide would indeed result in the observed 90 Da loss. There are two pathways which can lead to this loss. The first involves hydrogen atom attack at the β-carbon, as shown in Scheme 4b. The β-carbon position in amino acids is not predicted to have a high hydrogen atom affinity, because a pentavalent carbon intermediate is created, which mitigates the likelihood of this mechanism. Alternatively, a hydrogen deficient radical starting from the α-position of the amino acid is able to rearrange and produce the 90 Da side chain loss as shown in Scheme 4c. The α-position is known to stabilize hydrogen deficient radicals due to the captodative effect.[51,54,56,57] The results in Figure 1 clearly demonstrate that the 90 Da loss mechanism in Scheme 4c is favorable; however, further

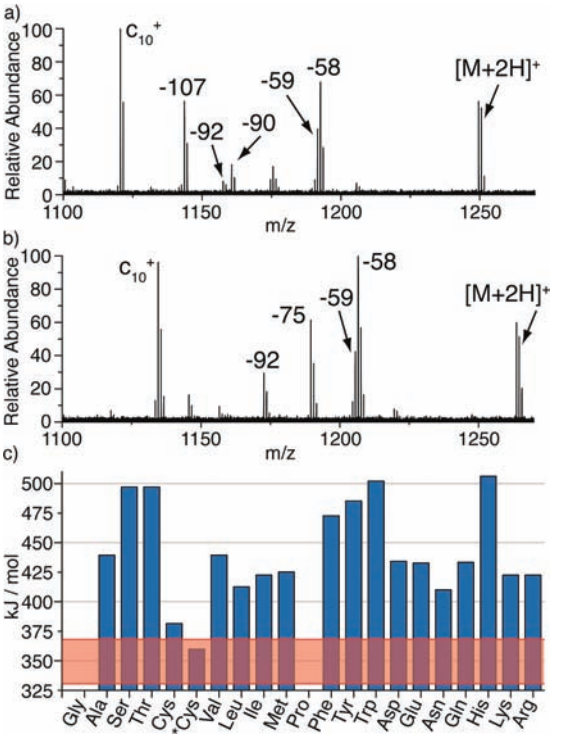

Figure 2. (a) ECD spectrum of the peptide YVDIAIPcGNK. (b) ECD spectrum of the peptide YVDIAIPc*GNK, where c* denotes α-methylcysteine. (c) BDEs of the products resulting from α-radical driven side chain dissociation from standard amino acids and the nonstandard amino acid *S*-cysteine-acetamide. The red region is the BDE range of amino acid α-hydrogens.

experiments are needed to prove that the same pathway is operative in ECD. In order to probe this issue experimentally, two peptides with the sequence YVDIAIPcGNK were prepared, one of them containing an α-methylcysteine variant. The α-methyl group should block the pathway outlined in Scheme 4c (because the abstracted hydrogen is replaced with a methyl group) while leaving the pathway in Scheme 4b open. The results in Figure 2a illustrate that the expected loss of 90 Da is observed in the standard peptide. In Figure 2b however, the α-methyl variant does not exhibit a loss of 90 Da, confirming that this fragmentation proceeds via the mechanism outlined in Scheme 4c in ECD experiments.

If hydrogen deficient radicals access the α-positions of amino acids following electron capture, radical conversion, and migration, then why is dissociation at modified cysteine observed while other comparable side chain losses are not? The most plausible hypothesis relates to the stability of the products, which is known to influence transition state energies in hydrogen deficient radical dissociation. The BDEs for all possible side chain losses that can occur from the α-radical initiation are shown in Figure 2c. The range of BDEs for all α-radicals is highlighted in red.[54] Only the loss of modified cysteine yields a radical which is comparable in stability to the α-radicals. All other side chain losses are therefore predicted to be significantly endothermic and disfavored. When taken as a whole, it is clear that consideration of the relevant energetics from a hydrogen deficient radical chemistry perspective explains both the favorable loss of 90 Da from modified cysteine and the absence of other equivalent side chain losses from the remaining amino acids.

dx.doi.org/10.1021/ja1096804 |*J. Am. Chem. Soc.* 2011, 133, 6997–7006

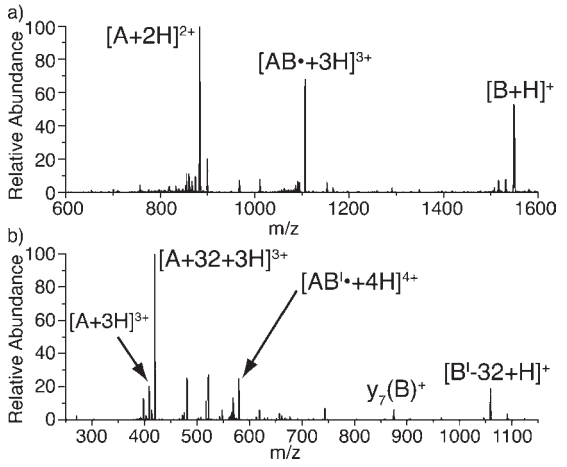

Figure 3. (a) PD/CID of the disulfide-bound peptides (A) VCYDKSFPISHVR and (B) RPHERNGFTVLCPKN. (b) PD/CID of the disulfide-bound peptides (A) SLRRSSCFGGR and (B) CDPGYIGSR.

Disulfide Bonds. The specific cleavage of disulfide bonds by ECD is a well-known process which is thought to occur via one of two pathways: direct electron capture into an antibonding orbital of the disulfide bond or hydrogen atom attack at one of the sulfur atoms.[3,11] Both of these mechanisms may be occurring in ECD, but a hydrogen deficient radical pathway also exists and may contribute to the observed disulfide cleavage products. The singly disulfide bound complex resulting from combination of the peptides RPHERNGFTVLCPKN and VCYDKSFPISHVR (iodinated at tyrosine) was subjected to photodissociation to generate a hydrogen deficient radical system. Collisional activation of the radical product is shown in Figure 3a. Cleavage of the disulfide bond leads to the major products. Again, the highly dominant disulfide dissociation is likely due to favorable structural features which place the disulfide and nascent radical in close proximity. When the even-electron peptide complex is subjected to CID, no disulfide dissociation is observed. For comparison, a similar experiment with the peptides SLRRSSCFGGR and CDPGYIGSR (iodinated at tyrosine) is shown in Figure 3b. In this case, dissociation at the disulfide is less dominant and is accompanied by related losses stemming from cleavage of the C−S bond adjacent to the disulfide. The hydrogen deficient pathways which lead to these products are shown in Scheme 5. Cleavage of the disulfide bond can be initiated from attack at the β-position or directly at the disulfide.[58] In contrast, dissociation of the C−S bond is initiated from the more stable α-position. The data in Figure 3 clearly confirms that both pathways are possible in hydrogen deficient radical peptides. Both types of dissociation are also observed in actual ECD experiments.[3] Given that we have established that hydrogen deficient radicals are generated in ECD experiments, it is likely that some portion of the dissociation observed at disulfide bonds occurs via the pathways outlined in Scheme 5. The observed preference for dissociation at disulfide bonds in ECD may be due to the existence of multiple feasible fragmentation pathways.

Origin of Hydrogen Deficient Radical Chemistry in ECD. The dissociation products observed in ECD from leucine, *S*-cysteine-acetamide, and disulfide bonds are consistent with pathways that would be expected from hydrogen deficient radical chemistry. Some of the observed fragmentations do not have plausible hydrogen abundant radical pathways, such as the loss of 56 Da from leucine. It is therefore reasonable to conclude that a significant population of the radicals in charge-reduced parent ions of ECD are converted to hydrogen deficient radials. We will now discuss the mechanisms by which hydrogen deficient radicals are created in ECD.

Scheme 5. Hydrogen Deficient Radical Disulfide Fragmentation: (a) Disulfide Bond Cleavage; (b) C−S Bond Dissociation

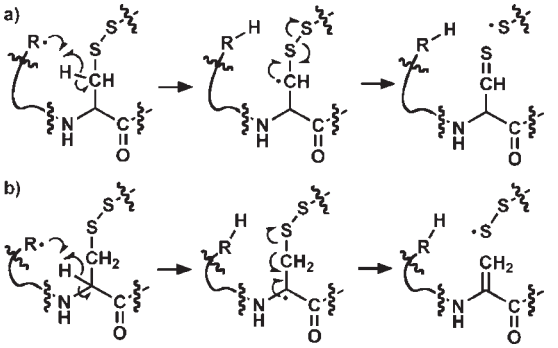

Direct Electron Capture at Charged Sites. NH_3 loss can occur promptly after direct electron capture and is a commonly observed dissociation in ECD experiments. Loss of NH_3 concomitantly converts the peptide to a hydrogen deficient state, leaving behind a radical at the point of dissociation.[17] It is not surprising, therefore, to note that all of the NH_3 accompanied side chain losses listed in Table 1 are readily explained in terms of hydrogen deficient chemistry. Importantly, NH_3-accompanied side chain losses in ECD experiments represent a substantial fraction of the total listed in Table 1; therefore, many of the side chain losses observed in ECD clearly occur via hydrogen deficient chemistry, but this fact is cloaked by the loss of NH_3, which shifts the masses from the equivalent losses on the right side of Table 1.

If direct electron capture occurs on a doubly charged tryptic peptide, the most likely sites for capture are arginine, lysine, and the N-terminus. Direct electron capture at protonated lysine is shown in Scheme 6a. A hydrogen abundant radical species is created in the form of a hypervalent $-NH_3$ group. A similar result will be produced by direct electron capture at the N-terminus. In contrast, direct electron capture at a protonated arginine residue, as shown in Scheme 6b, yields a hydrogen deficient radical species directly via a loss of a degree of saturation in the guanidinium moiety. This conversion has been noted previously in quantum mechanical structure calculations.[59] The capacity of arginine to convert directly to a hydrogen deficient radical should lead to observable differences in the dissociation patterns for arginine-containing peptides versus lysine-containing peptides if there is a competition between hydrogen abundant and hydrogen deficient radical chemistry as postulated herein. The extent to which this difference is observable will also be influenced by the process of H atom loss.

Following direct electron capture, conversion to an even-electron species is possible through the loss of an H atom for arginine, lysine, and the N-terminus. The even-electron product left behind by H atom loss no longer contains a radical and thus cannot undergo subsequent radical chemistry. Hydrogen atom loss from the charge-reduced ion is commonly observed in ECD.

Scheme 6. (a) Protonated Lysine and (b) Protonated Arginine Side Chains after Direct Electron Capture at the Charge Site

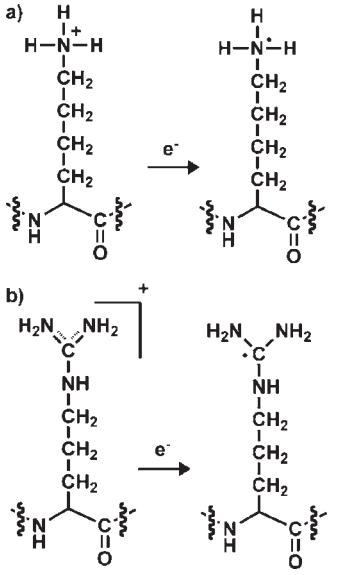

One factor that strongly influences H atom loss is peptide size,[1] which is demonstrated in Figure 4a. The size effect can be rationalized in a generic fashion by consideration of peptide structure. For doubly charged peptides, shorter sequences will exhibit less intramolecular charge solvation due to increased Coulombic repulsion relative to longer peptides. The results in Figure 4a clearly indicate that as charge solvation becomes more favorable in larger peptides, H atom loss is observed less frequently. This further suggests that persistence of the products formed in Scheme 6 likely requires significant charge solvation, perhaps to remove energy released from the electron capture event or to facilitate hydrogen atom transfer.

The pathway shown in Scheme 6b implies that arginine may be less susceptible to H atom loss than lysine because arginine can directly access a hydrogen deficient state. Figure 4b shows the individual and averaged values of the ratio of charge reduced to H atom loss intensity as a function of peptide size for arginine- and lysine-containing peptides from the ECD database. Although the predominance of z ions in the database suggests that charge capture at the N-terminus may occur more commonly than at lysine or arginine, a clear trend is still observed. The results demonstrate that arginine-containing peptides are less likely to undergo H atom loss compared to lysine, particularly for larger peptides. As a control, a similar analysis was performed for alanine and glycine, which are residues not associated with direct electron capture. No difference is observed between alanine and glycine, as shown in Figure 4c (the statistical sampling breaks down for the largest peptides due to low numbers). These results suggest that the pathway in Scheme 6b is one viable route by which electron capture can lead to a hydrogen deficient state.

Radical Conversion at the Peptide Backbone. The product generated by direct electron capture at lysine shown in Scheme 6a can be converted into a hydrogen deficient radical by several routes. Scheme 2c depicts hydrogen atom transfer from a hydrogen abundant moiety to a backbone carbonyl on a peptide. This isobaric conversion from a hydrogen abundant to a hydrogen deficient radical involves loss of a degree of saturation

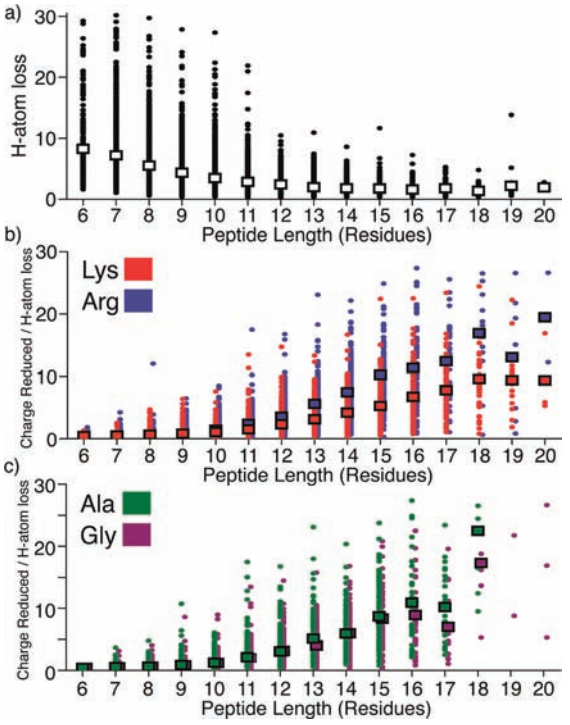

Figure 4. (a) Abundance of hydrogen atom side chain loss as a function of peptide length. The hydrogen atom loss is shown as the fractional abundance relative to the precursor ion. Each peptide is represented as a data point. Histograms for (b) arginine- and lysine-containing peptides and (c) alanine- and glycine-containing peptides. Ratios of charge-reduced parent ion abundance versus hydrogen atom loss after electron capture are plotted as a function of peptide length. In all plots the average values for each peptide length are shown as large squares.

and forms an aminoketyl radical structure. The aminoketyl radical has been extensively studied by many groups as the proposed immediate precursor to $c/z^{\bullet}$ ion formation; however, the radical structure is hydrogen deficient and is also theoretically capable of hydrogen abstraction. The calculated BDE of the aminoketyl radical structure, 365 kJ/mol, is higher than the average α-position BDE of ~350 kJ/mol, which suggests that radical migration from the aminoketyl to an α-position would be a reasonable process. Direct synthesis of this radical structure in the gas phase would therefore be extremely useful in answering questions about the propensity of radical migration versus $c/z^{\bullet}$ formation from the aminoketyl radical. Hydrogen deficient radical peptides naturally dissociate via pathways which generate aminoketyl-like radical structures, as shown in Scheme 7.

Figure 5a shows the CID of an aminoketyl radical generated by the C-terminal pathway shown in Scheme 7c for the peptide RPPGYSPFR. A significant amount of c_8 ion is formed at the C-terminus, in agreement with the anticipated dissociation site for the aminoketyl radical shown in Scheme 7c. Hydrogen deficient radical initiated side chain losses such as 86 and 99 Da from arginine are also observed in significant abundance. The fragment ions a_5 and a_8 are also products typical of hydrogen deficient backbone dissociation due to radical migration to the β-positions of aromatic residues in the peptide.[41] Finally, the c_5 fragment is related to an aminoketyl mechanism through serine, which does not have an isolatable intermediate.[41] Similar results are obtained with aminoketyl radicals generated in peptides by the mechanisms shown in Scheme 7a,b, although the relative

dx.doi.org/10.1021/ja1096804 |*J. Am. Chem. Soc.* 2011, 133, 6997–7006

Scheme 7. The Three Pathways Which Can Generate Aminoketyl Radicals by Radical Migration: (a) Aspartic Acid Pathway I; (b) Aspartic Acid Pathway II; (c) C-Terminal Pathway

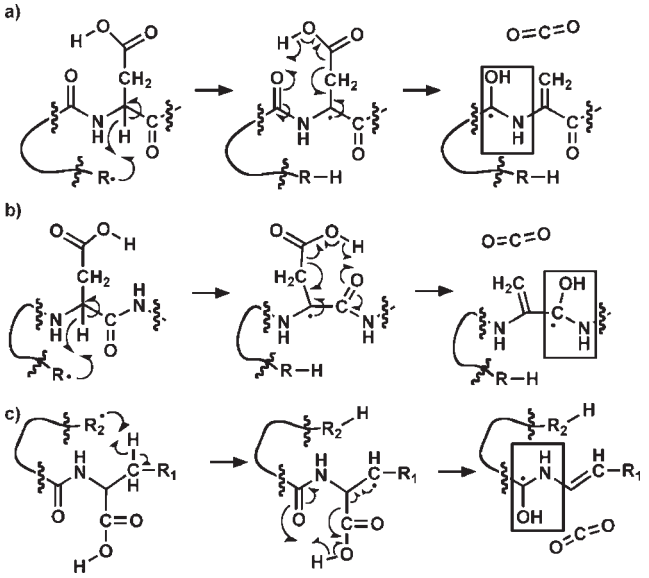

amount of c/z• type dissociation that is observed is reduced. Importantly, c/z• ions are observed adjacent to the expected location of the aminoketyl radical in every case. The relative yields of c/z• ion formation versus hydrogen deficient radical migration observed in Figure 5a and similar experiments are not in agreement with results obtained in ECD, where the formation of c/z• ions typically dominates.

As stated above, the products in Scheme 7 are similar to, but not identical with, the aminoketyl radicals generated in ECD. The primary difference relates to the presence of dehydroalanine. As noted previously,[60] dehydroalanine allows delocalization of the radical produced by the pathway in Scheme 7b and interferes with c/z• ion product formation for the aminoketyl radicals generated by the pathways in Scheme 7a,c. Therefore, it is not surprising that modulation of the aminoketyl radical chemistry enables additional hydrogen deficient radical migration to occur. In order to confirm the relevance of the results in Figure 5a, we conducted further experiments to determine if the presence of dehydroalanine would influence actual ECD experiments. In Figure 5b the side chain loss region of the ECD spectrum for a phosphoserine-containing peptide is shown. Typical c/z• fragmentation is observed elsewhere in the spectrum, and most of the side chain losses correspond to hydrogen abundant pathways, as can be seen in Table 1. Figure 5c shows the ECD spectrum for the same peptide where the phosphoserine has been chemically converted to dehydroalanine. Hydrogen deficient side chain losses from the parent ion such as 99 and 86 Da from arginine along with 56 and 43 Da from leucine are observed and match by exact mass with those given for hydrogen deficient processes in Table 1. A significant decrease in c/z• ion formation in the dehydroalanine-containing peptide was also observed. These results suggest that modulation of the aminoketyl radical can influence the propensity of this intermediate to undergo c/z• ion formation versus radical migration. It is worth noting that structural effects due to the absence of phosphate may also contribute to the observed differences in dissociation in Figure 5.

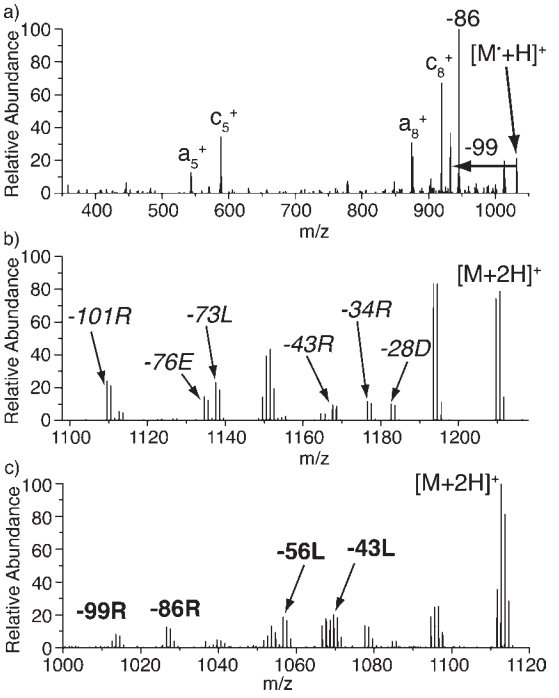

Figure 5. (a) CID of the aminoketyl radical product from PD/CID of the peptide RPPGY[1]SPFR. (b) ECD side chain loss data for RLEAsLADVR; hydrogen abundant initiated losses are shown in italics. (c) ECD side chain loss data for RLEAdLADVR; hydrogen deficient losses are shown in boldface. The lower case "s" represents phosphorylated serine, and "d" represents dehydroalanine.

It is likely that peptide sequence, location of charges, hydrogen-bonding networks, and other factors influence the microenvironment for each potential aminoketyl radical in a peptide. Similarly, it is likely that some fraction of these aminoketyl radicals will undergo migration and are therefore a potential source of hydrogen deficient chemistry observed in ECD.

Radical Conversion at Amino Acid Side Chains. Hydrogen atom transfer to the amide side chains of glutamine and asparagine (as noted previously),[61] and *S*-cysteine-acetamide produces radical structures similar to the aminoketyl backbone radical shown in Scheme 1. Analysis of the fragmentation of these side chains is therefore directly relevant to the backbone dissociation typically observed in ECD. As shown in Table 1, analysis of the SwedECD database reveals that 47.1% of Asn-containing peptides yield a side chain loss of 59 Da following hydrogen atom transfer, as shown in Scheme 8a. This pathway is highly analogous to backbone dissociation, which produces c/z• ions. Although a similar mechanism can be drawn for glutamine as shown in Scheme 8b, only 5.6% of peptides containing glutamine actually exhibit this loss. The disparity can be rationalized by the stabilities of the nascent radicals. For asparagine, a highly stabilized α-radical is the product, whereas for glutamine a much less stable primary carbon radical is generated. The calculated transition state energies for the pathways in Scheme 8a,b are also in excellent agreement with the experimental observations. The transition state energy for asparagine is ~46 kJ/mol, and the loss is somewhat endothermic (ΔH = 37 kJ/mol) due to disruption of hydrogen bonding with the side chain. In contrast, the transition state energy for glutamine is ~103 kJ/mol and the reaction is endothermic by 137 kJ/mol.

dx.doi.org/10.1021/ja1096804 |*J. Am. Chem. Soc.* 2011, 133, 6997–7006

Scheme 8. Hydrogen Atom Attack at (a) Asn, (b) Gln, and (c) *S*-Cys-Acetamide

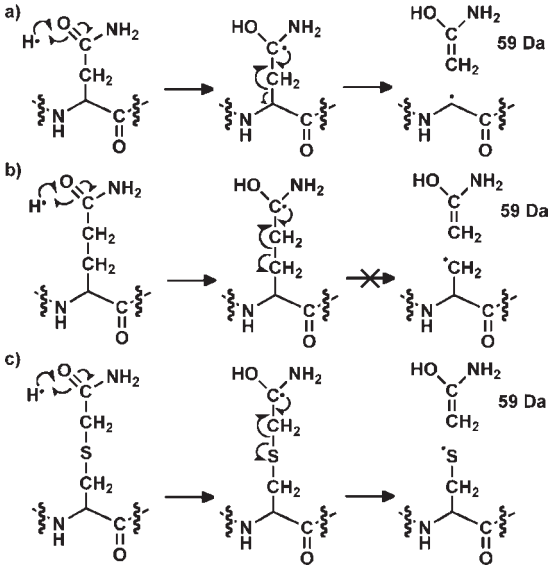

Scheme 9. Hydrogen Atom Attack at (a) Asp and (b) Glu

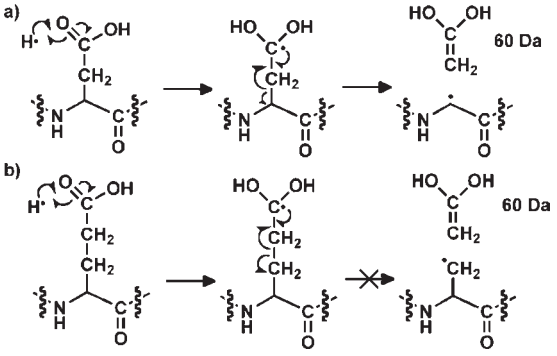

This rationale is further supported by the observation that the same loss of 59 Da from *S*-cysteine-acetamide occurs with 43.2% regularity and produces a stable sulfur radical[62] as the product. These observations are in excellent agreement with the trends observed for backbone dissociation with the introduction of dehydroalanine into peptides as shown in Figure 5: i.e., dissociation from an aminoketyl radical can be inhibited by destabilizing the radical product.

A closely related side chain loss of 60 Da can occur for aspartic and glutamic acid, as shown in Scheme 9. The relative frequencies are 60.4% and 1.0%, respectively. Again, the results can be rationalized in terms of the stabilities of the radical products.[63] Although side chain dissociation is disfavored in the cases of Glu and Gln, a stable radical species is formed on the carbonyl carbon, which may then undergo hydrogen deficient radical migration. The initially formed side chain radicals have calculated BDEs of 371 kJ/mol for Glu and 356 kJ/mol for Gln, which are both expected to be able to migrate to lower energy α-radical positions. These radicals are likely formed on Glu and Gln in high abundance (on the basis of the amount of dissociation observed for Asp and Asn) and are likely sources of subsequent hydrogen deficient radical chemistry in peptides containing these residues.

Charge remote electron capture at acidic sites (such as the side chains of glutamic and aspartic acid) has not been evaluated previously and may differ substantially from capture at amide sites. It is therefore unknown presently whether charge remote capture analogous to what is predicted at backbone amide sites would be feasible for the side chains of Glu and Asp. Regardless of whether such charge remote capture is subsequently shown to be unlikely, the results can still be rationalized on the basis that Glu and Asp side chains are excellent hydrogen bond partners and are therefore likely to be solvating charges in peptides. This would make them likely targets for H atom attack following electron capture at a protonated site. Indeed, hints of such behavior can be observed in statistical analysis of ECD fragmentation.[64]

CONCLUSION

Many pathways exist for the conversion of hydrogen abundant radicals to hydrogen deficient radicals in ECD. This conversion is the key to understanding a number of side chain losses which are not readily explained by hydrogen abundant processes alone. Side chain losses such as −56 Da from leucine and −90 Da from *S*-cysteine-acetamide in ECD point to both the creation and migration of hydrogen deficient radicals in the charge reduced parent ion. Examination of the SwedECD database also shows that hydrogen deficient side chain losses are regularly observed after a radical conversion process has taken place, such as the neutral loss of NH_3. The propensity of hydrogen atom loss from the charge-reduced parent ion in ECD is directly related to the ability of a hydrogen abundant species to convert to a hydrogen deficient species. As expected, the amount of hydrogen atom loss is therefore dependent on the structure of the charge site as well as the length of the peptide in which it resides. From this information it can be concluded that electron capture can lead directly to a hydrogen deficient species or an initially formed hydrogen abundant radical may quickly convert to a hydrogen deficient radical, which then dictates much of the subsequent observed chemistry that leads to dissociation.

ASSOCIATED CONTENT

Supporting Information. Figures giving Asn and Glu transition state structures and text giving the full citation for ref 52. This material is available free of charge via the Internet at http://pubs.acs.org.

AUTHOR INFORMATION

Corresponding Author
ryan.julian@ucr.edu

ACKNOWLEDGMENT

We thank Joe Loo for instrument time at UCLA to acquire the ECD data. We thank Jack Simons, Jack Beauchamp, Evan Williams, Julia Laskin, and Frank Turecek for helpful discussions. This work was supported by funds from the National Science Foundation (No. CHE-0747481).

REFERENCES

(1) Zubarev, R. A.; Kelleher, N. L.; McLafferty, F. W. *J. Am. Chem. Soc.* **1998**, *120*, 3265–3266.
(2) Syka, J. E. P.; Coon, J. J.; Schroeder, M. J.; Shabanowitz, J.; Hunt, D. F. *Proc. Natl. Acad. Sci. U.S.A.* **2004**, *101*, 9528–9533.
(3) Zubarev, R. A.; Kruger, N. A.; Fridriksson, E. K.; Lewis, M. A.; Horn, D. M.; Carpenter, B. K.; McLafferty, F. W. *J. Am. Chem. Soc.* **1999**, *121*, 2857–2862.
(4) Guan, Z. Q.; Kelleher, N. L.; OConnor, P. B.; Aaserud, D. J.; Little, D. P.; McLafferty, F. W. *Int. J. Mass Spectrom.* **1996**, *158*, 357–364.
(5) Zubarev, R. A.; Horn, D. M.; Fridriksson, E. K.; Kelleher, N. L.; Kruger, N. A.; Lewis, M. A.; Carpenter, B. K.; McLafferty, F. W. *Anal. Chem.* **2000**, *72*, 563–573.
(6) Kelleher, R. L.; Zubarev, R. A.; Bush, K.; Furie, B.; Furie, B. C.; McLafferty, F. W.; Walsh, C. T. *Anal. Chem.* **1999**, *71*, 4250–4253.
(7) Annan, R. S.; Carr, S. A. *J. Protein Chem.* **1997**, *16*, 391–402.
(8) Zubarev, R. *Expert Rev. Proteomics* **2006**, *3*, 251–261.
(9) Swaney, D. L.; McAlister, G. C.; Coon, J. J. *Nat. Methods* **2008**, *5*, 959–964.
(10) Sohn, C. H.; Chung, C. K.; Yin, S.; Ramachandran, P.; Loo, J. A.; Beauchamp, J. L. *J. Am. Chem. Soc.* **2009**, *131*, 5444–5459.
(11) Anusiewicz, W.; Berdys-Kochanska, J.; Simons, J. *J. Phys. Chem. A* **2005**, *109*, 5801–5813.
(12) Pouthier, V.; Tsybin, Y. O. *J. Chem. Phys.* **2008**, *129* (9), 095106.
(13) Breuker, K.; Oh, H. B.; Lin, C.; Carpenter, B. K.; McLafferty, F. W. *Proc. Natl. Acad. Sci. U.S.A.* **2004**, *101*, 14011–14016.
(14) Turecek, F. *J. Am. Chem. Soc.* **2003**, *125*, 5954–5963.
(15) Zubarev, R. A.; Haselmann, K. F.; Budnik, B.; Kjeldsen, F.; Jensen, F. *Eur. J. Mass Spectrom.* **2002**, *8*, 337–349.
(16) Savitski, M. M.; Nielsen, M. L.; Zubarev, R. A. *Anal. Chem.* **2007**, *79*, 2296–2302.
(17) Falth, M.; Savitski, M. M.; Nielsen, M. L.; Kjeldsen, F.; Andren, P. E.; Zubarev, R. A. *Anal. Chem.* **2008**, *80*, 8089–8094.
(18) Cooper, H. J.; Hudgins, R. R.; Hakansson, K.; Marshall, A. G. *J. Am. Soc. Mass Spectrom.* **2002**, *13*, 241–249.
(19) Laskin, J.; Yang, Z. B.; Lam, C.; Chu, I. K. *Anal. Chem.* **2007**, *79*, 6607–6614.
(20) Leymarie, N.; Costello, C. E.; O'Connor, P. B. *J. Am. Chem. Soc.* **2003**, *125*, 8949–8958.
(21) Li, X. J.; Cournoyer, J. J.; Lin, C.; O'Connor, P. B. *J. Am. Soc. Mass Spectrom.* **2008**, *19*, 1514–1526.
(22) Chung, T. W.; Turecek, F. *J. Am. Soc. Mass Spectrom.* **2010**, *21* (8), 1279–1295.
(23) Ly, T.; Julian, R. R. *J. Am. Chem. Soc.* **2008**, *130*, 351–358.
(24) Diedrich, J. K.; Julian, R. R. *Anal. Chem.* **2010**, *82*, 4006–4014.
(25) Reed, D. R.; Hare, M.; Kass, S. R. *J. Am. Chem. Soc.* **2000**, *122*, 10689–10696.
(26) Budnik, B. A.; Haselmann, K. F.; Zubarev, R. A. *Chem. Phys. Lett.* **2001**, *342*, 299–302.
(27) Anusiewicz, I.; Jasionowski, M.; Skurski, P.; Simons, J. *J. Phys. Chem. A* **2005**, *109*, 11332–11337.
(28) Ly, T.; Yin, S.; Loo, J. A.; Julian, R. R. *Rapid Commun. Mass Spectrom.* **2009**, *23*, 2099–2101.
(29) Hao, G.; Gross, S. S. *J. Am. Soc. Mass Spectrom.* **2006**, *17*, 1725–1730.
(30) Masterson, D. S.; Yin, H. Y.; Chacon, A.; Hachey, D. L.; Norris, J. L.; Porter, N. A. *J. Am. Chem. Soc.* **2004**, *126*, 720–721.
(31) Hodyss, R.; Cox, H. A.; Beauchamp, J. L. *J. Am. Chem. Soc.* **2005**, *127*, 12436–12437.
(32) Chu, I. K.; Rodriguez, C. F.; Rodriguez, F.; Hopkinson, A. C.; Siu, K. W. M. *J. Am. Soc. Mass Spectrom.* **2001**, *12*, 1114–1119.
(33) Barlow, C. K.; Moran, D.; Radom, L.; McFadyen, W. D.; O'Hair, R. A. J. *J. Phys. Chem. A* **2006**, *110*, 8304–8315.
(34) Kalcic, C. L.; Gunaratne, T. C.; Jonest, A. D.; Dantus, M.; Reid, G. E. *J. Am. Chem. Soc.* **2009**, *131*, 940–942.
(35) O'Connor, P. B.; Lin, C.; Cournoyer, J. J.; Pittman, J. L.; Belyayev, M.; Budnik, B. A. *J. Am. Soc. Mass Spectrom.* **2006**, *17*, 576–585.
(36) Han, H. L.; Xia, Y.; McLuckey, S. A. *J. Proteome Res.* **2007**, *6*, 3062–3069.
(37) Chung, T. W.; Turecek, F. *J. Am. Soc. Mass Spectrom.* **2010**, *21*, 1279–1295.
(38) Tsybin, Y. O.; He, H.; Emmett, M. R.; Hendrickson, C. L.; Marshall, A. G. *Anal. Chem.* **2007**, *79*, 7596–7602.
(39) Ben Hamidane, H.; Chiappe, D.; Hartmer, R.; Vorobyev, A.; Moniatte, M.; Tsybin, Y. O. *J. Am. Soc. Mass Spectrom.* **2009**, *20*, 567–575.
(40) Savitski, M. M.; Kjeldsen, F.; Nielsen, M. L.; Zubarev, R. A. *J. Am. Soc. Mass Spectrom.* **2007**, *18*, 113–120.
(41) Sun, Q. Y.; Nelson, H.; Ly, T.; Stoltz, B. M.; Julian, R. R. *J. Proteome Res.* **2009**, *8*, 958–966.
(42) Moore, B. N.; Blanksby, S. J.; Julian, R. R. *Chem. Commun.* **2009**, *33*, 5015–5017.
(43) Ly, T.; Julian, R. R. *J. Am. Soc. Mass Spectrom.* **2009**, *20*, 1148–1158.
(44) Turecek, F.; Syrstad, E. A. *J. Am. Chem. Soc.* **2003**, *125*, 3353–3369.
(45) Ly, T.; Julian, R. R. *J. Am. Chem. Soc.* **2010**, *132*, 8602–8609.
(46) Syrstad, E. A.; Turecek, F. *J. Am. Soc. Mass Spectrom.* **2005**, *16*, 208–224.
(47) Sobczyk, M.; Anusiewicz, W.; Berdys-Kochanska, J.; Sawicka, A.; Skurski, P.; Simons, J. *J. Phys. Chem. A* **2005**, *109*, 250–258.
(48) Regoeczi, E. *Iodine-labeled Plasma Proteins*; CRC Press: Boca Raton, FL, 1984.
(49) Chan, W. C.; White, P. D. *Fmoc Solid Phase Peptide Synthesis: A Practical Approach*; Oxford University Press: New York, 2004.
(50) Sechi, S.; Chait, B. T. *Anal. Chem.* **1998**, *70*, 5150–5158.
(51) Klemm, C.; Schroder, S.; Gluckmann, M.; Beyermann, M.; Krause, E. *Rapid Commun. Mass Spectrom.* **2004**, *18*, 2697–2705.
(52) Tam, J. P.; Wu, C. R.; Liu, W.; Zhang, J. W. *J. Am. Chem. Soc.* **1991**, *113*, 6657–6662.
(53) Frisch, M. J.; *Gaussian 03, Revision D.01*; Gaussian, Inc., Wallingford, CT, 2004.
(54) Rauk, A.; Yu, D.; Taylor, J.; Shustov, G. V.; Block, D. A.; Armstrong, D. A. *Biochemistry* **1999**, *38*, 9089–9096.
(55) Peng, C. Y.; Schlegel, H. B. *Isr. J. Chem.* **1993**, *33*, 449–454.
(56) Viehe, H. G.; Janousek, Z.; Merenyi, R.; Stella, L. *Acc. Chem. Res.* **1985**, *18*, 148–154.
(57) Hopkinson, A. C. *Mass Spectrom. Rev.* **2009**, *28*, 655–671.
(58) Sohn, C. H.; Kim, T.-Y.; Beauchamp, J. L. . *Conference on Ion Chemistry and Mass Spectrometry*, Lake Arrowhead, CA, Jan 14−16, 2011.
(59) Panja, S.; Nielsen, S. B.; Hvelplund, P.; Turecek, F. *J. Am. Soc. Mass Spectrom.* **2008**, *19*, 1726–1742.
(60) Chung, T. W.; Turecek, F. *Int. J. Mass Spectrom.* **2011**, *301* (1−3), 55–61.
(61) Haselmann, K. F.; Budnik, B. A.; Kjeldsen, F.; Polfer, N. C.; Zubarev, R. A. *Eur. J. Mass Spectrom.* **2002**, *8*, 461–469.
(62) Rauk, A.; Yu, D.; Armstrong, D. A. *J. Am. Chem. Soc.* **1998**, *120*, 8848–8855.
(63) Li, X. J.; Lin, C.; O'Connor, P. B. *Anal. Chem.* **2010**, *82*, 3606.
(64) Savitski, M. M.; Kjeldsen, F.; Nielsen, M. L.; Zubarev, R. A. *Angew. Chem., Int. Ed.* **2006**, *45*, 5301–5303.